Electrochemical Oxidation of Aliphatic Amines and Their Attachment to Carbon and Metal Surfaces

ARTICLE *in* LANGMUIR · OCTOBER 2004

Impact Factor: 4.46 · DOI: 10.1021/la049194c · Source: PubMed

5 AUTHORS, INCLUDING:

Mohamed Chehimi
Institut de Chimie et des Matériaux Paris-Est
269 PUBLICATIONS **5,444** CITATIONS
SEE PROFILE

Jean Pinson
Paris Diderot University
163 PUBLICATIONS **7,687** CITATIONS
SEE PROFILE

Electrochemical Oxidation of Aliphatic Amines and Their Attachment to Carbon and Metal Surfaces

Alain Adenier,[‡] Mohamed M. Chehimi,[‡] Iluminada Gallardo,*[,†] Jean Pinson,[§] and Neus Vilà[†]

Departament de Química, Universitat Autònoma de Barcelona, Bellaterra, España, ITODYS, Université Paris 7-Denis Diderot, 75005 Paris, France, and Laboratoire d'Electrochimie Moléculaire, Université Paris 7-Denis Diderot, 75251 Paris Cedex 05, France

Received March 29, 2004. In Final Form: July 1, 2004

The electrochemical oxidation of aliphatic amines (primary, secondary, and tertiary) has been investigated by cyclic voltammetry and preparative electrolysis. The oxidation mechanisms have been established, and the lifetimes of the radical cations have been measured for secondary and tertiary amines. These results have been put in parallel with the attachment of amines to glassy carbon, Au, and Pt electrodes by cyclic voltammetry, X-ray photoelectron spectroscopy (XPS), and infrared reflection−absorption spectroscopy (IRRAS). It is then possible to show that it is not the radical cation but the radical obtained after the deprotonation which reacts with the electrode surface. XPS results also point to the existence of a covalent bond between Au or Pt and the organic moiety.

Introduction

The electrochemical oxidation of aromatic amines has been widely investigated, as, upon oxidation, they polymerize to give conducting polymers such as polyanilines.[1a] The polymerization is due to the coupling of radical cations.[1b,c] However, in the great majority of cases (except for primary aromatic amines), the process stops at a less condensed level. Dimerization is observed, giving rise to the formation of C−C bonds (benzidines), C−N bonds (phenylamines), or N−N bonds (hydrazines). For example, *N*,*N*-dimethylaniline dimerizes upon electrochemical oxidation to give benzidine (Scheme 1). The mechanism involves the carbon−carbon coupling of two radical cations as the rate determining step.[2a,b]

However, in the oxidation of alkylarylamines in the presence of a base, the rate determining step is the deprotonation of the radical cation which evolves by a disproportionation.[2c−f] In some cases, such as tris-(4-bromo or methoxy)phenylamine, stable radical cations are observed.[3]

With aromatic amines, the electrochemical oxidation mostly involves radical cations, as exemplified in Scheme 1, and the covalent attachment to the electrode surface upon oxidation has never been observed.

Aliphatic amines are more difficult to oxidize and give rise to unstable intermediates due to the lack of delocalization of the charge. They have been much less investigated, and the classical papers on this topic go back to the 1960s.[4] The mechanism proposed by Mann[4a,b] for tertiary amines is shown in Scheme 2.

Scheme 1

Scheme 2

$$(RCH_2CH_2)_3N - 1e^- \longrightarrow (RCH_2CH_2)_3\overset{\bullet+}{N}$$

$$(RCH_2CH_2)_3\overset{\bullet+}{N} \longrightarrow (RCH_2CH_2)_2N\overset{\bullet}{C}HCH_2R + H^+$$

Path A:

$$(RCH_2CH_2)_2N\overset{\bullet}{C}HCH_2R - 1e^- \longrightarrow (RCH_2CH_2)_2N\overset{+}{C}HCH_2R$$

$$(RCH_2CH_2)_2N\overset{+}{C}HCH_2R + H_2O \longrightarrow (RCH_2CH_2)_2NH + RCH_2CHO + H^+$$

Path B:

$$2(RCH_2CH_2)_2N\overset{\bullet}{C}HCH_2R \longrightarrow (RCH_2CH_2)_3N + (RCH_2CH_2)_2NCH{=}CHR$$

$$(RCH_2CH_2)_2NCH{=}CHR + H_2O \longrightarrow (RCH_2CH_2)_2NH + RCH_2CHO$$

Global Reaction

$$(RCH_2CH_2)_3N - 2e^- + H_2O \longrightarrow (RCH_2CH_2)_2NH + RCH_2CHO + 2H^+$$

Scheme 3

$$2(RCH_2CH_2)_3N - 2e^- + H_2O \longrightarrow (RCH_2CH_2)_2\overset{+}{N}H_2 + (RCH_2CH_2)_3\overset{+}{N}H + RCH_2CHO$$

The oxidation leads to a radical cation which deprotonates to give a radical. Then, two paths are opened for this radical, either an oxidation to an iminium cation (path A) or a dismutation to an amine and an enamine (path B). In both ways, the overall reaction provides a secondary amine, an aldehyde, and protons. This proton would protonate a starting amine to give an electrochemically inactive ammonium ion, and the reaction would consume, as observed by cyclic voltammetry (CV) and electrolysis, one electron per starting molecule (Scheme 3).

Upon the oxidation of secondary amines, the formation of primary amines was observed, while primary amines

[†] Universitat Autònoma de Barcelona.

[‡] ITODYS, Université Paris 7-Denis Diderot.

[§] Laboratoire d'Electrochimie Moléculaire, Université Paris 7-Denis Diderot.

(1) (a)*Handbook of Conductive Polymers*; Skotheim, T. A., Elsenbaumer, R. L., Reynolds, J. R., Eds.; Marcel Dekker: New York, 1988. (b) Geniès, E. M.; Boyle, A.; Lapkowski, M.; Tsintavis, C. *Synth. Met.* **1990**, *36*, 139. (c) Yang, H.; Bard, A. J. *J. Electroanal. Chem.* **1992**, *339*, 423.

(2) (a)Larumbe, D.; Gallardo, I.; Andrieux, C. *J. Electroanal. Chem.* **1991**, *304*, 241. (b) Larumbe, D.; Moreno, M.; Gallardo, I.; Bertrán J.; Andrieux, C. P. *J. Chem. Soc., Perkin Trans. 2* **1991**, *1437*. (c) Andrieux, C. P.; Gallardo, I.; Junca, M. *J. Electroanal. Chem.* **1993**, *354*, 231. (d) Serve, D. *Electrochim. Acta* **1976**, *21*, 1171. (e) Cauquis, G.; Cognard, J.; Serve, D. *Electrochim. Acta* **1975**, *20*, 101. (f) Dinnocenzo, J. P.; Banach, T. E. *J. Am. Chem. Soc.* **1989**, *111*, 8646.

(3) Seo, E. T.; Nelson, R. F.; Fritsch, J. M.; Marcoux, L. S.; Leedy, D. W.; Adams, R. F. *J. Am. Chem. Soc.* **1966**, *88*, 3498.

(4) (a) Mann, C. K.; Barnes, K. K. *Electrochemical Reactions in Nonaqueous Systems*; Marcel Dekker: New York, 1970. (b) Portis, L. C.; Bhat, V. V.; Mann, C. K. *J. Org. Chem.* **1970**, *35*, 2175. (c) Ross, S. D. *Tetrahedron Lett.* **1973**, 1237.

10.1021/la049194c CCC: $27.50
Published on Web 08/17/2004

Scheme 4

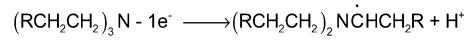

Scheme 5

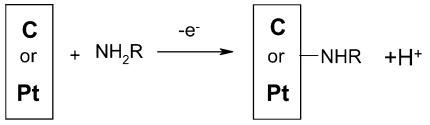

formed ammonia and nitrogen.[4] This mechanism has been criticized by Ross.[4c] He pointed out that, in the case of benzyldimethylamine or dibenzylmethylamine where the formation of the enamine is not possible, the dealkylation process still takes place and benzaldehyde is still obtained. In this case, the first process through the iminium cation would be the only one possible. The formation of the immonium cation from benzhydryl dimethylamine has been fully documented in acetonitrile on a Pt electrode.[5] However, a question arises of the same existence of the radical cation, as a concerted electron transfer cleavage reaction could as well be possible (Scheme 4). A different mechanism has been observed for tri-*iso*-propylamine;[6] the cyclic voltammogram is reversible down to 0.05 V s^{-1}. The conformation of the stable radical cation was determined: the $C_\alpha-H$ bond is in the NC_3 plane.

More recently, it was found that the oxidation of amines could lead to the attachment of an organic group to the surface of a carbon electrode,[7] and it was proposed that the nitrogen was bonded to the surface, as shown in Scheme 5.

Attachment to the surface was demonstrated by cyclic voltammetry, X-ray photoelectron spectroscopy (XPS), and secondary-ion mass spectrometry (SIMS). By the oxidation of pure ethylenediamine and other ω-diamines on a Pt electrode, the formation of polyethyleneimine[8] (and analogues) was characterized by an electrochemical quartz microbalance and infrared reflection−absorption spectroscopy (IRRAS). A mechanism was proposed for the growth of the polymer film.

Other electrografting reactions are known: the reduction of activated olefins on metals,[9] the reduction of diazonium salts on carbon[10a−e] or iron electrodes,[10f−h] the oxidation of aryl acetates on carbon electrodes,[11] the oxidation of hydrazides on carbon in a manner similar to that of amines,[12] the oxidation of alcohols on carbon,[13] and the reaction of hydrogen radicals with carbon surfaces.[14] For all these electrografting reactions, radicals have been proposed as the species responsible for the attack of the surface. The only exception is the grafting of alcohols where it has been proposed that the carbon itself is oxidized.

Scheme 6

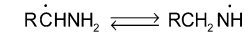

Concerning this oxidative grafting mechanism of amines, some conclusions have been attained in previous investigations: (i) path A of Scheme 2 has been considered as the way to the formation of linear polyimine obtained by the oxidation on Pt of pure ethylenediamine;[8] (ii) cleavage of the C−N bond was never observed in the different compounds examined; for example, after grafting 2-amino thiazole, the sulfur atom can be observed by XPS, and the nitro groups of 4-nitrobenzylamine[7a] and the anthracene group of anthrylmethylamine[7a] can be observed by cyclic voltammetry; (iii) it was found by XPS[7b] that the attachment of primary amines (butylamine) is rather easy but that the surface coverage by secondary amines (*N*-methylbutylamine and *N*-ethylbutylamine) was less than half that of primary amines and that tertiary amines (*N*,*N*-dimethylbutylamine and triethylamine) are not attached at a detectable level to the carbon surface; these differences were assigned to differences of steric hindrance at the level of the radical cation; (iv) By examination of the electricity consumption during the grafting of ethylenediamine, the radical cations were responsible for the attachment to the electrode surface.[7a] However, as indicated above, with the exception of the oxidation of alcohols, all the other known reactions are due to the reactivity of radicals and, in this oxidative grafting mechanism of amines, the intermediate radical of Scheme 6 in equilibrium with its tautomeric amino radical could be the key reagent in the attachment reaction.

It is the aim of this paper to reexamine in more detail the grafting mechanism of aliphatic amines to electrode surfaces through a detailed investigation of the behavior of different amines: Is it the radical cation or the ensuing radical which is responsible for the grafting of the organic moiety? A related question is the same existence of the radical cation, as a concerted electron transfer cleavage reaction could as well be possible (Scheme 4).

To come as close as possible to this goal, we shall put in parallel, for different aliphatic amines (primary, secondary, or tertiary), the electrochemical behavior (cyclic voltammetry and electrolysis) and the description (electron

(5) (a) Andrieux, C. P.; Savéant, J. M. *Bull. Soc. Chim. Fr*. **1968**, 4671. (b) Andrieux, C. P.; Savéant, J. M. *Bull. Soc. Chim. Fr*. **1969**, 1254.

(6) Bock, H.; Goebel, I.; Havlas, Z.; Liedle, S.; Oberhammer, H. *Angew. Chem*. **1991**, *30*, 187.

(7) (a) Barbier, B.; Pinson, J.; Desarmot, G.; Sanchez, M. *J. Electrochem. Soc*. **1990**, *137*, 1757. (b) Deinhammer, R. S.; Ho, M.; Anderegg, J. W.; Porter, M. D. *Langmuir* **1994**, *10*, 1306. (c) Downard, A. J. *Electroanalysis* **2000**, *12*, 1085.

(8) (a) Herlem, G.; Goux, C.; Fahys, B.; Dominati, F.; Gonçalvès, A. M.; Penneau, J. F. *J. Electroanal. Chem*. **1997**, *435*, 259. (b) Herlem, G.; Reybier, K.; Trokourey, A.; Fahys, B. *J. Electrochem. Soc*. **2000**, *147*, 597. (c) Lakard, B.; Herlem, G.; Fahys, B. *J. Chem. Phys*. **2001**, *115*, 7219. (d) Lakard, B.; Herlem, G.; Fahys, B. *THEOCHEM* **2002**, *584*, 15. (e) Lakard, B.; Herlem, G.; Fahys, B. *THEOCHEM* **2002**, *593*, 133. (f) Lakard, B.; Herlem, G.; Fahys, B. *THEOCHEM* **2003**, *638*, 177.

(9) (a) Lécayon, G.; Bouizem, Y.; Le Gressus, C.; Reynaud, C.; Boiziau, C.; Juret, C. *Chem. Phys. Lett*. **1982**, *91*, 506−510. (b) Deniau, G.; Lécayon, G.; Bureau, C.; Tanguy, J. In *Protective Coatings and Thin Films*; Pauleau, Y., Barna, P. B., Eds.; Kluwer Academic: Amsterdam, The Netherlands, 1997; pp 265−278. (c) Viel, P.; Bureau, C.; Deniau, G.; Zalczer, G.; Lécayon, G. *J. Electroanal. Chem*. **1999**, *470*, 14 and references therein.

(10) (a) Delamar, M.; Hitmi, R.; Pinson, J.; Savéant, J. M. *J. Am. Chem. Soc*. **1992**, *114*, 588. (b) Allongue, P.; Delamar, M.; Desbat, B.; Fagebaume, O.; Hitmi, R.; Pinson, J.; Savéant, J. M. *J. Am. Chem. Soc*. **1997**, *119*, 588. (c) Delamar, M.; Desarmot, G.; Fagebaume, O.; Hitmi, R.; Pinson, J.; Savéant, J. M. *Carbon* **1997**, *35*, 801. (d) Coulon, E.; Pinson, J.; Bourzat, J.-D.; Commerçon, A.; Pulicani, J.-P. *Langmuir* **2001**, *17*, 7102. (e) Coulon, E.; Pinson, J.; Bourzat, J.-D.; Commerçon, A.; Pulicani, J.-P. *J. Org. Chem*. **2002**, *67*, 8515. (f) Adenier, A.; Bernard, M.-C.; Chehimi, M. M.; Deliry, E.; Desbat, B.; Fagebaume, O.; Pinson, J.; Podvorica, F. *J. Am. Chem. Soc*. **2001**, *123*, 4541. (g) Chaussé, A.; Chehimi, M. M.; Karsi, N.; Pinson, J.; Podvorica, F.; Vautrin-Ul, C. *Chem. Mater*. **2002**, *14*, 392. (h) Adenier, A.; Cabet-Deliry, E.; Lalot, T.; Pinson, J.; Podvorica, F. *Chem Mater*. **2002**, *14*, 4576. (i) Andrieux, C. P.; Pinson, J. *J. Am. Chem. Soc*. **2003**, *125*, 14801.

(11) (a) Andrieux, C. P.; Gonzalez, F.; Savéant, J. M. *J. Am. Chem. Soc*. **1997**, *119*, 4292. (b) Geneste, F.; Moinet, C.; Jezequel, G. *New J. Chem*. **2002**, *26*, 1539. (c) Geneste, F.; Moinet, C.; Jezequel, G. *New J. Chem*. **2002**, *26*, 1539.

(12) (a) Norwall, W. B.; Wipf, D. O.; Kuhr, W. G. *Anal. Chem*. **1998**, *70*, 2601. (b) Hayes, M. A.; Kuhr, W. G. *Anal. Chem*. **1999**, *71*, 1720.

(13) (a) Maeda, H.; Yamauchi, Y.; Hosoe, M.; Li, T. X.; Yamaguchi, E.; Kamatsu, M.; Ohmori, H. *Chem. Pharm. Bull*. **1994**, *42*, 1870. (b) Maeda, H. Y.; Li, T. X.; Hosoe, M. *Anal. Sci*. **1994**, *10*, 963. (c) Maeda, H.; Hosoe, M.; Li, T. X.; Yamaguchi, E.; Ohmori, H. *Anal. Sci*. **1995**, *11*, 947. (d) Maeda, H.; Itami, M.; Yamauchi, Y.; Ohmori, H. *Chem. Pharm. Bull*. **1996**, *44*, 2294. (e) Maeda, H.; Kitano, T.; Huang, C. Z.; Katayama, K. *Anal. Sci*. **1999**, *15*, 531.

(14) Kuo, T. C.; McCreery, R. L. *Anal. Chem*. **1999**, *71*, 1553.

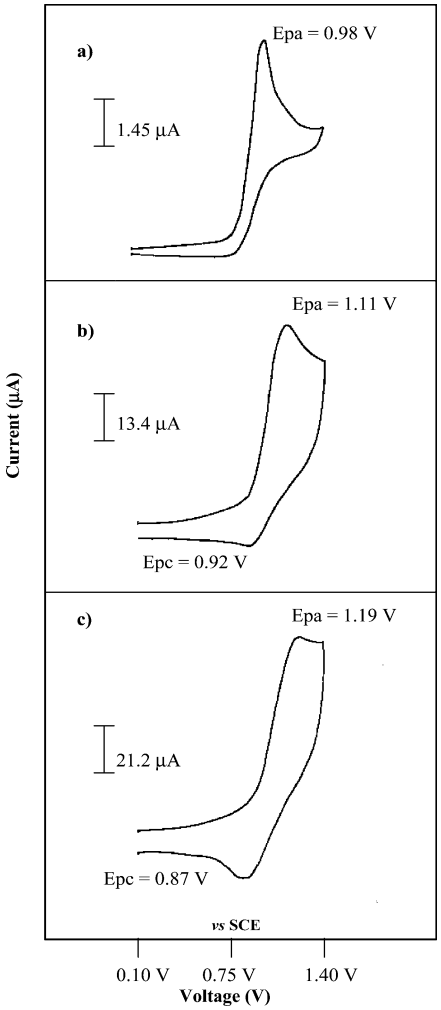

Figure 1. Cyclic voltammogram of tri-*iso*-butylamine (**5**) (c = 4.1 mM) in DMF + 0.1 M NBu_4BF_4 on a glassy carbon electrode (d = 1 mm) at (a) 0.1, (b) 10, and (c) 30 V s^{-1}. Reference SCE.

Scheme 7

	R_3N		R_2NH		RNH_2	
R	$-CH_2CH_3$	1	$-(CH_2)_2CH_3$	6	$-(CH_2)_3CH_3$	12
	$-(CH_2)_2CH_3$	2	$-CH_2CH(CH_3)_2$	7	$-(CH_2)_5CH_3$	13
	$-(CH_2)_3CH_3$	3	$-CH_2CH(CH_2CH_3)((CH_2)_3CH_3)$	8	$-C_6H_{11}$	14
	$-(CH_2)_4CH_3$	4	$-C_6H_{11}$	9	$-C(CH_3)_3$	15
	$-CH_2CH(CH_3)_2$	5	$-CH(CH_3)CH_2CH_3$	10		
			$-CH(CH_3)_2$	11		

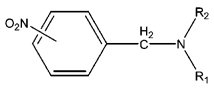

4-nitro	$R_1 = R_2 = H$	16
3-nitro	$R_1 = R_2 = H$	17
	$R_1 = CH_3, R_2 = H$	18
	$R_1 = R_2 = CH_3$	19

transfer properties, XPS, and IRRAS analysis) of the electrode surface obtained after electrolysis of the amine.

The amines that have been examined are shown in Scheme 7, and the amines attached to carbon or metal will be termed by the name of the metal and the number of the amine, for example, ***Pt*16**.

Results

Attachment of amines to carbon and metal surfaces takes place in acetonitrile (ACN); as this reaction proceeds, the surface becomes passivated. As a result, on the second scan, the wave shifts and decreases. After maintaining the potential at the peak of the wave, it even disappears,

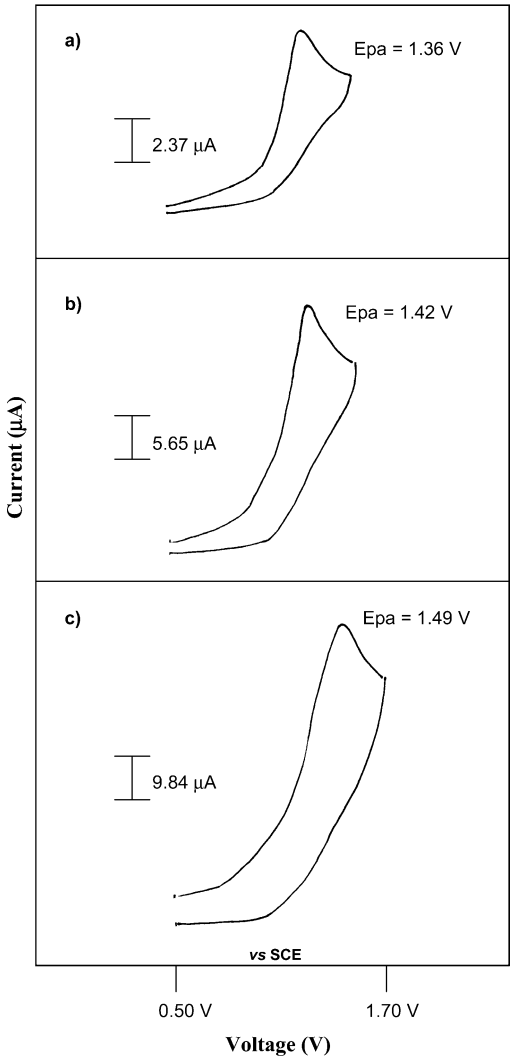

Figure 2. Cyclic voltammogram of *n*-butylamine (**12**) (c = 5.5 mM) in DMF + 0.1 M NBu_4BF_4 on a glassy carbon electrode (d = 1 mm) at (a) 0.1, (b) 1.0, and (c) 10 V s^{-1}.

as shown in the passivation of the electrode section (Figure 3). This is always observed during electrochemical grafting experiments and constitutes a clear indication of such a reaction. Under such conditions, it is not possible to gather significant electrochemical data. The following experiments have therefore been performed in dimethylformamide (DMF), a solvent in which the experiments are more reproducible. Furthermore, the aliphatic amines are stronger bases in ACN than in DMF.

Electrochemical Behavior of Tertiary Amines. Tri-*iso*-butylamine (**5**) (Figure 1) shows on a glassy carbon electrode in DMF + 0.1 M NBu_4BF_4 a single irreversible one-electron wave at 0.98 V/SCE, the width of which is 65 mV. The peak potential is independent of the concentration, and by increasing the scan rate (v) up to 30 V s^{-1}, the voltammetric peak becomes partly reversible.

The standard potential can be deduced as the midpoint between cathodic and anodic peaks, $E° = 1.01 \pm 0.01$ V/SCE. Analysis of the peak potential, at low and high scan rates, indicates a one-electron process (by comparison of $I_p c^{-1} v^{-1/2}$ with the monoelectronic wave of tris-(4-bromophenylamine)). In the 4.0−8.0 mM range, the peak potential is concentration independent (<10 mV by unit log c) and scan rate dependent (50 mV by unit log v at low scan rates and 100 mV by unit log v at high scan rates). These values suggest a mixed kinetic control at low scan

Scheme 8

$$[(CH_3)_2CHCH_2]_3N - 1e^- \longrightarrow [(CH_3)_2CHCH_2]_3N^{\bullet+} \quad E^0, k_s^{ap}, \alpha$$

$$[(CH_3)_2CHCH_2]_3N^{\bullet+} \longrightarrow \text{PRODUCTS} \quad k$$

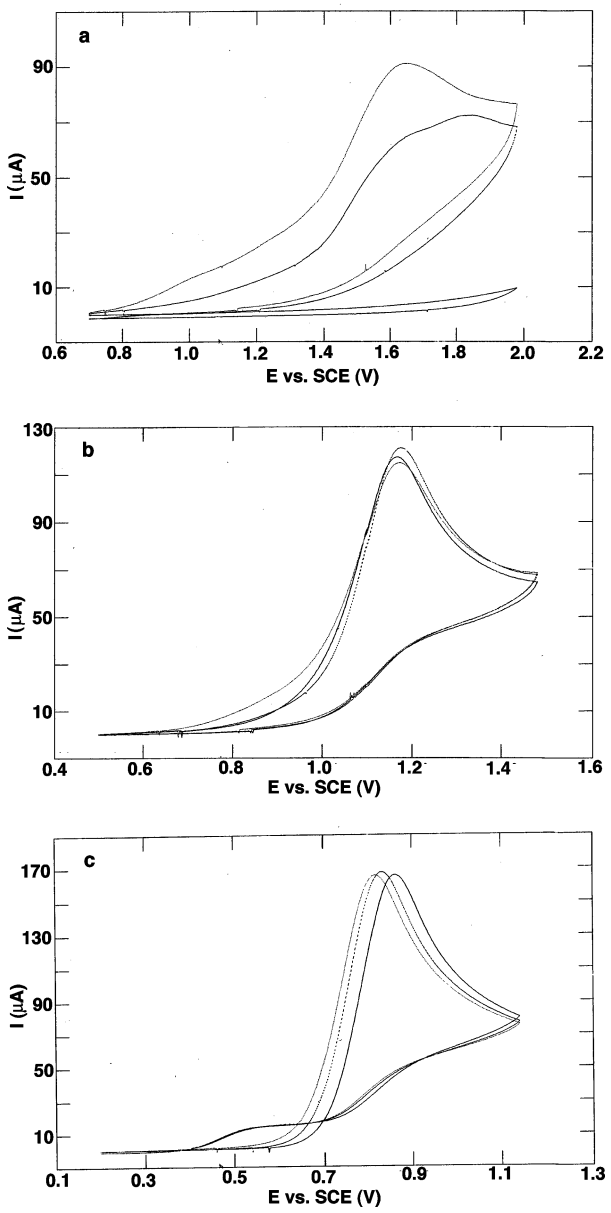

Figure 3. Cyclic voltammetry of the first, second, and third scans of (a) *n*-butylamine, (b) di-*n*-butylamine, and (c) tri-*n*-butylamine (recorded after maintaining for 300 s a potential 300 mV more positive than the peak potential in a 5.0 mM solution of the amine in ACN + 0.1 M NBu_4BF_4. Glassy carbon electrode, $v = 0.2$ V s^{-1}, reference SCE.

rates and a kinetic control by electron transfer at high scan rates. This behavior is indicative of an EC process (electron transfer followed by a chemical reaction) (see Scheme 8).

Further analysis and simulation[15] of the voltammogram (see Supporting Information S1: Analysis of the Voltammogram of Tri-*iso*-butylamine (**5**)) allows determination of the different parameters.

(15) Rudolf, M.; Feldberg, S. W. *DigiSim 2.0*; cyclic voltammetric simulator for Windows; Bioanalytical Systems Inc.: West Lafayette, IN, 1996.

Table 1. Electrochemical Data, Obtained by DigiSim Simulation of the Experimental Cyclic Voltammograms, for Tertiary Aliphatic Amines[a]

amine	E_{pa}[b,c]	$E°$[c]	ΔE_{pa}[b,d]	n	α	k_s^{app}[e]	k[f]	mechanism
tri-*iso*-butylamine (**5**)	0.98	1.00	65	1	0.5	7×10^{-3}	50	EC
tri-*n*-pentylamine (**4**)	0.91	0.90	80	1	0.5	3×10^{-3}	50	EC
tri-*n*-butylamine (**3**)	0.88	0.87	80	1	0.5	4×10^{-3}	60	EC
tri-*n*-propylamine (**2**)	0.95	0.94	80	1	0.5	2×10^{-3}	90	EC
triethylamine (**1**)	0.94	0.99	90	1	0.5	7×10^{-3}	100	EC

[a] The measurements are given in Supporting Information S1 for **5**. [b] At 0.1 V s^{-1}. [c] In V/SCE. [d] In mV. [e] In cm s^{-1}. [f] In s^{-1}.

The values in Table 1 are in good agreement, and the differences lie within experimental errors. Electrolysis of **5** was performed to determine the oxidation products: After consumption of 0.72 F (a consumption of 1 F would be expected from the cyclic voltammetry), the current decreases to nearly 0 mA and a voltammogram of the final solution indicates the absence of oxidizable products. After neutralization and extraction with toluene, it is possible to observe (GC−MS and cyclic voltammetry) the presence of tri-*iso*-butylamine (**5**) (14% yield) and of di-*iso*-butylamine (**7**) (46% yield), 30% of the products being lost in the extraction process. The fact that **5** and **7**, which are oxidizable, cannot be observed by cyclic voltammetry in the final electrolysis solution indicate that they are protonated at the end of the electrolysis and deprotonated during the final workup. Di-*iso*-butylamine (**7**) is not observed at the end of the process because it is formed after the treatment with a basic aqueous solution. The overall reaction can be written as shown in Scheme 9, with isopropaldehyde being lost in the extraction process. From the cyclic voltammetry data and the results of the electrolysis, the mechanism shown in Scheme 10 can be established for **5**. Other tertiary aliphatic amines have been investigated by cyclic voltammetry and preparative electrolysis. The electrochemical data are gathered in Table 1.

They all follow the same EC mechanism where a relatively stable radical cation (lifetime of $\sim(7-14) \times 10^{-3}$ s) deprotonates and leads to a radical in the second step. At the end of the process, the expected secondary amines are obtained in all cases.

Electrochemical Behavior of Secondary Amines. We will examine the amines of type $(RCH_2)_2NH$ or $(R_1R_2CH)_2NH$. The amines with a hydrogen α of the nitrogen behave similarly to tertiary amines. At 0.1 V s^{-1}, they show a monoelectronic irreversible oxidation peak with a width of 95 mV, and a partial reversibility can be observed at $v = 30$ or 40 V s^{-1}. The voltammograms can be analyzed along the same lines as above, and the thermodynamic and kinetic parameters are gathered in Table 2.

Controlled potential electrolysis was performed on dicyclohexylamine ($c = 17.0$ mM and $E_{app} = +1.08$ V/SCE) in DMF + 0.1 M $LiClO_4$; at the end of the process, the solution was treated with a basic aqueous solution to deprotonate the amines and extract them with toluene. A GC−MS analysis indicated the presence of the starting material (55%) and 10% cyclohexanone. Cyclohexylamine

Scheme 9

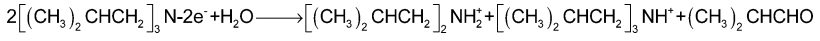

Scheme 10

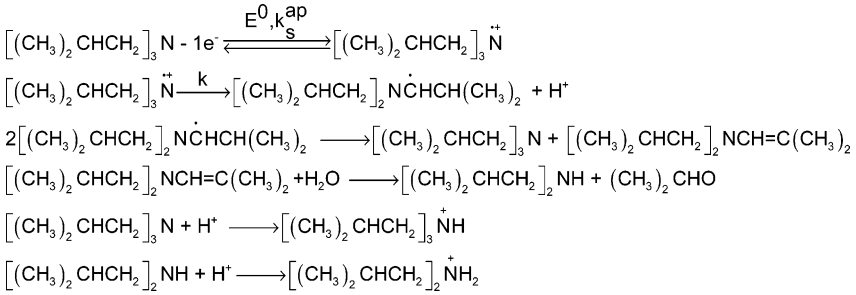

Table 2. Electrochemical Data, Obtained by DigiSim Simulation of the Experimental Cyclic Voltammograms, for Secondary Aliphatic Amines $(RCH_2)_2NH$ and $(R_1R_2CH)_2NH$[a]

amine	E_{p_a}[a,b]	$E°$ [b]	ΔE_{p_a}[a,c]	n	α	k_s^{app} [d]	k[e]	mechanism
di-*n*-butylamine (**6**)	1.11	1.12	95	1	0.5	3×10^{-3}	150	EC
di-*iso*-butylamine (**7**)	1.11	1.10	95	1	0.5	3×10^{-3}	120	EC
bis-2-ethylhexylamine (**8**)	1.07	1.07	95	1	0.5	3.5×10^{-3}	120	EC
dicyclohexylamine (**9**)	1.06	1.06	95	1	0.5	4.6×10^{-3}	165	EC
di-*sec*-butylamine (**10**)	1.16	1.18	95	1	0.5	4×10^{-3}	165	EC
di-*iso*-propylamine (**11**)	1.15	1.17	95	1	0.5	4.5×10^{-3}	165	EC

[a] At 0.1 V s^{-1}. [b] In V/SCE. [c] In mV. [d] In cm s^{-1}. [e] In s^{-1}.

Table 3. Electrochemical Data, Obtained by DigiSim Simulation of the Experimental Cyclic Voltammograms, for Primary Aliphatic Amines[a]

amine	E_{p_a}[b,c]	ΔE_{p_a}[b,d]	α	n
n-butylamine (**12**)	1.36	110	0.4	1
tert-butylamine (**15**)	1.44	95	0.5	1
n-hexylamine (**13**)	1.36	110	0.4	1
cyclohexylamine (**14**)	1.39	105	0.5	1

[a] The measurements are given in Supporting Information S2 for **12**. [b] At 0.1 V s^{-1}. [c] In V/SCE. [d] In mV.

was probably lost during the separation procedure, and the large amount of remaining starting material can likely be assigned to the protonation of cyclohexylamine or to the blocking of the electrode.

The similarity of the voltammograms between the tertiary amines and secondary amines **6**−**11** indicates that a mechanism similar to that of Scheme 10 is operative, the main differences being a somewhat more difficult oxidation as could be expected from the donating effect of the alkyl groups and a slightly faster loss of a proton.

Electrochemical Behavior of Primary Amines. The electrochemical investigation of these amines is much more difficult due to their strong propensity to attach to the electrode even in DMF, and careful polishing of the electrode between every measurement is mandatory. The voltammogram of *n*-butylamine (**12**) is presented in Figure 2.

The monoelectronic wave of **12** is irreversible up to 100 V s^{-1}. The transfer coefficient (α) can be measured from the width of the peak, and as observed in Table 3, it does not differ very much from 0.5. As the reversibility cannot be attained, it is not possible to determine the other parameters.

For primary amines, the radical cations are much more unstable than those for the other amines and their lifetime is shorter than 0.2 ms, but the values of α always close to 0.5 do not indicate an electron transfer concerted with the follow-up reaction.

Grafting of the Electrodes. Figure 3 shows the cyclic voltammetry (first and second cycle) for tri-, di-, and mono-*n*-butylamines in ACN; the voltammograms were recorded after maintaining for 300 s a potential 300 mV more positive than the voltammetric peak potential. Under these conditions, for tertiary and secondary amines, the height of the oxidation peak of the second and third cycle is about the same at that of the first scan. However, in the case of the primary *n*-butylamine (**12**), the electrode is completely blocked. This indicates that the grafting reaction is much more efficient with primary amines.

Table 4. Differences of Peak Potentials (ΔE_p Values)[a] for Reversible Systems on Modified Electrodes

	substituent of the grafted amino group[b]	tris-4-bromo-phenylamine[c]	4-nitro-toluene[c]	$K_3Fe(CN)_6$[d]
C	*n*-butyl (**12**)	180	184	∞[e]
	n-hexyl (**14**)	227	244	∞
	di-*n*-butyl (**6**)	130	153	∞
	tri-*n*-butyl (**3**)	78	95	200
	none	70	93	150
Au	*n*-butyl (**12**)	113	200	138
	n-hexyl (**14**)	105	185	105
	di-*n*-butyl (**6**)	103	163	120
	tri-*n*-butyl (**3**)	72	90	102
	none	60	85	80
Pt	*n*-butyl (**12**)	104	400	∞
	n-hexyl (**14**)	115	304	∞
	di-*n*-butyl (**6**)	93	157	147
	tri-*n*-butyl (**3**)	66	75	90
	none	68	73	75

[a] In mV on glassy carbon (d = 3 mm), Au (d = 1 mm), and Pt electrodes (d = 1 mm). [b] Grafting was achieved by maintaining the potential at the peak potential of the amine for 300 s in a 5.0 mM solution of the amine in ACN + 0.1 M NBu_4BF_4. [c] 10.0 mM solution of the compound in ACN + 0.1 M NBu_4BF_4. [d] 10.0 mM $K_3Fe(CN)_6$ in aqueous 0.1 M KCl solution. [e] The curves are drawn out with ΔE_p > 850 mV.

Binding of an organic layer to the surface of the electrode slows down the electron transfer and increases the difference of peak potentials (ΔE_p) of a reversible system in solution.[16] A simple estimation of the rate of electron transfer is therefore given by the difference of potentials between the cathodic and anodic peaks of a reversible monoelectronic system.[17] ΔE_p increases from 60 mV for a fast electron transfer to higher values as the electron transfer slows down. Table 4 presents the values of ΔE_p

(16) Duvall, S. H.; McCreery, R. L. *Anal. Chem.* **1999**, *71*, 4594.
(17) (a) Bard, A. J.; Faulkner, L. R. *Electrochemical Methods*; Wiley: New York, 2001; p 242. (b) Nicholson, R. S. *Anal. Chem.* **1965**, *37*, 1351.

Table 5. Electrochemical Data of Nitrobenzylamines[a]

	oxidation			reduction
amine	E_{p_a}[b] DMF	E_{p_a}[b] ACN	reversibility oxidation wave[c]	$E°$[b,e] ACN
4-nitrobenzylamine (**16**)	1.42	1.58	irrev[d]	−1.15
3-nitrobenzylamine (**17**)	1.51	1.78	irrev[d]	−1.14
N-methyl-3-nitrobenzylamine (**18**)	1.25	1.33	40	−1.14
N,*N*-dimethyl-3-nitrobenzylamine (**19**)	1.01	1.07	10	−1.12

[a] On a glassy carbon electrode ($d = 3$ mm). [b] In V/SCE. [c] Scan rate (in V s^{-1}) at which the reversibility is observed. [d] No reversibility is observed up to 200 V s^{-1}. [e] Standard reduction potential of the nitrobenzylamines.

Table 6. Surface Concentration of Glassy Carbon, Gold, and Platinum Electrodes Modified by the Oxidation of Nitrobenzylamines

amine	electrolysis potential[a]	$E°$ of nitrophenyl groups[b]	Γ^c on glassy carbon	Γ^c on Au	Γ^c on Pt
4-nitrobenzylamine (**16**)	+1.7	−1.15	4.0×10^{-10}	*d*	6.1×10^{-10}
3-nitrobenzylamine (**17**)	+1.8	−1.14	6.4×10^{-10}	*d*	6.5×10^{-10}
N-methyl-3-nitrobenzylamine (**18**)	+1.4	−1.14	3.2×10^{-10}	6.5×10^{-10}	8.6×10^{-10}
N,*N*-dimethyl-3-nitrobenzylamine (**19**)	+1.3	−1.12	0[e]	0[e]	0[e]

[a] Electrolysis at peak potential (in V/SCE) of the amine; time, 30 min; concentration of the amine, 5.0 mM. [b] Nitrophenyl groups attached to the surface of glassy carbon. [c] Surface concentration of $\pm 0.5 \times 10^{-10}$ (in mol cm^{-2}). [d] Cannot be measured; the wave of the amine is positive compared to the background. [e] Negligible.

for two reversible systems in ACN, tris-4-bromophenylamine and 4-nitrotoluene, and one reversible system in water, potassium ferricyanide ($K_3Fe(CN)_6$). The values on a bare and on a modified (by electrolysis of primary, secondary, and tertiary amines) electrode are compared.

The electron transfer to tris-4-bromophenylamine on bare carbon, Au, and Pt electrodes appears to be fast, as ΔE_p is always close to 60 mV; the transfer is slower with 4-nitrotoluene (ΔE_p varies from 73 to 93 mV) and becomes very slow with ferricyanide in aqueous solution. With tris-4-bromophenylamine as a redox probe on a carbon electrode, there is a large increase of ΔE_p[17] from a bare electrode (rate of heterogeneous electron transfer of $k_s = 0.03_7$ cm s^{-1}) to an electrode modified by the oxidation of primary amines ($k_s = 0.002_7$ cm s^{-1} for butylamino groups attached to the surface and 0.001_1 cm s^{-1} for hexylamino groups). This difference of the rate of electron transfer is due to the attachment of the organic layer to the conductive surface. For a pure tunneling current, the rate of heterogeneous electron transfer (k_s) varies with the thickness of the layer in an exponential function: $k_s = k_s° \exp(-\beta d)$, where $k_s°$ is for an uncoated electrode, β is the tunneling parameter, and d is the thickness of the layer.[18] Values of β for alkyl chains of self-assembled monolayers (SAMs) of alkylthiol on Au ranging from 0.89 to 1.14 $Å^{-1}$ per CH_2 unit have been measured.[18] Thus, the d values in butyl- and hexylamines can be considered proportional to the number of CH_2 groups in the alkyl chain. This seems appropriate for these two related molecules. The k_s values are obtained from the simulation of the voltammograms using the values of ΔE_p of Table 4. The values of β which are obtained, $\beta = 0.3 \pm 0.1$ $Å^{-1}$ on carbon and 0.2 ± 0.1 $Å^{-1}$ on Au and Pt, are clearly lower than the values obtained with SAMs, indicating that another electron transfer path is available to the redox probe and that the layers are probably not pinhole free. The same conclusion can be reached using 4-nitrotoluene as a redox probe. With ferricyanide in an aqueous solution, the electron transfer becomes so slow and the curves so drawn out that it becomes impossible to measure the peak difference. In this case, the slowness of the electron transfer obviously stems from hydrophobic interaction between the alkyl layer and the probe in an aqueous solution. With secondary amines on carbon, the variation of ΔE_p by comparison with a bare electrode is smaller than that with primary amines (both with tris-4-bromophenylamine and 4-nitrotoluene), suggesting a lower coverage of the surface; this is also true on Au and Pt. With the tertiary amine, on carbon, Au, and Pt, the values of ΔE_p come close to the values obtained with untreated electrodes, indicating a very low surface concentration.

Another way of estimating the efficiency of the grafting reaction is to measure the surface concentration of the organic groups; this has been done[7a] with 4-nitrobenzylamine. We also examined the electrochemical behavior of nitrobenzylamines **16**, **17**, **18**, and **19** on glassy carbon in DMF and ACN (Table 5). The electrode, after surface modification, is carefully rinsed in an ultrasonic cleaner and transferred to a new solution containing only the solvent (ACN) and supporting electrolyte (0.1 M NBu_4BF_4). Scanning toward negative potentials, one can observe the reversible system of the grafted nitrophenyl group (Table 6), the standard potential of which can be determined; it is very close to that of the parent benzylamine (Table 5). The observation of this reversible system confirms the presence of nitrophenyl groups on the surface.

The surface concentration can be obtained by integration of the reversible reduction peak of the nitrobenzyl groups located at ~ -1.1 V/SCE. Table 6 shows the surface concentrations (Γ values) obtained for the different nitrobenzylamines. These values can be compared with those which can be calculated from molecular models[7] for a compact layer of **16** attached to a perfectly plane surface of $\Gamma = 6.8 \times 10^{-10}$ mol cm^{-2}. From these data, it is possible to conclude that grafting is observed with primary and secondary amines, leading to concentrations of the same order of magnitude, but that no grafting can be detected with the tertiary 3-nitrobenzyl-*N*,*N*-dimethylamine. The oxidation potential of 3- and 4-nitrobenzylamines on Au is too close to or more positive than the background limit, and it is therefore not possible to obtain reliable data on this metal.

XPS Analysis of Modified Electrodes. We examined glassy carbon, Au, and Pt electrodes modified by the oxidation of tri-*n*-butylamine (**3**), di-*n*-butylamine (**6**), and *n*-butylamine (**12**). Figure 4 displays the survey scans obtained at a 90° takeoff angle for **12** attached to a Au and a Pt surface, respectively. The peaks which are labeled on this figure correspond to the elements of interest for this study: the doublets at 84.0 and 87.7 eV ($Au4f_{7/2}$ and $Au4f_{5/2}$)

(18) (a) Finklea, H. O.; Hanshew, D. D. *J. Am. Chem. Soc.* **1992**, *114*, 3173. (b) Slowinski, K.; Slowinska, K. U.; Majda, M. *J. Phys. Chem. B* **1999**, *103*, 8544. (c) Slowinski, K.; Fong, H. K. Y.; Majda, M. *J. Am. Chem. Soc.* **1999**, *121*, 7257.

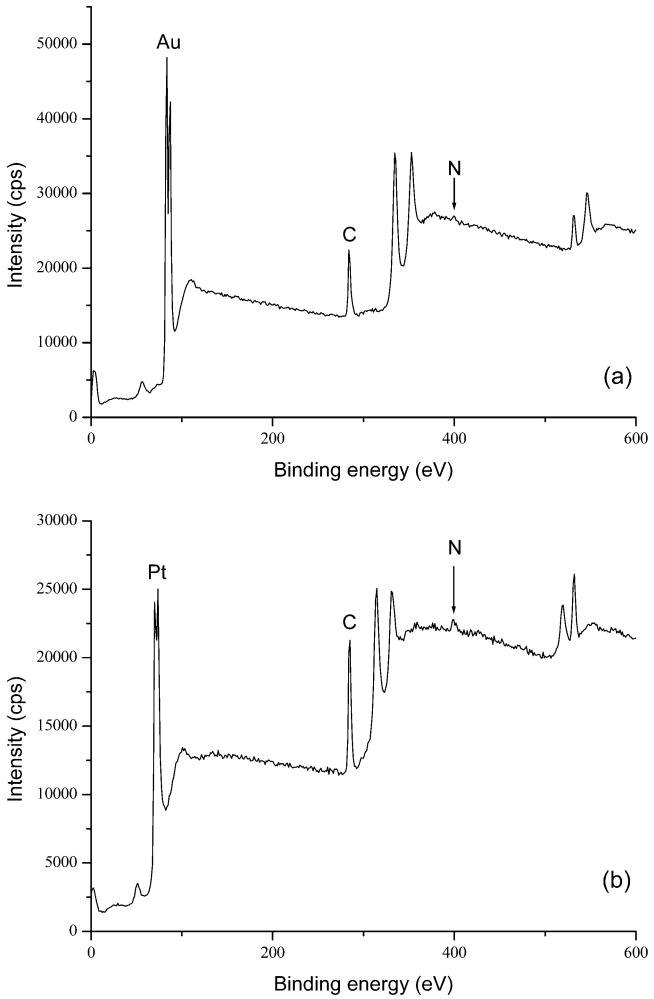

Figure 4. XPS survey scan of *n*-butylamine (**12**) grafted on (a) Au and (b) Pt. The main 4f doublets for Au and Pt are only indicated on the figure.

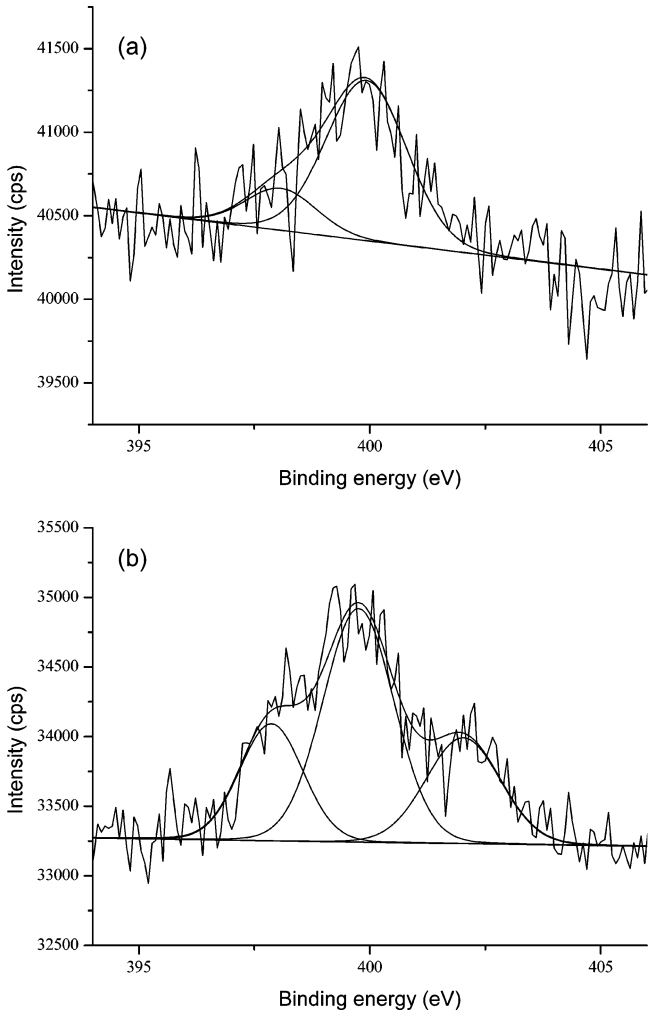

Figure 5. XPS spectra of the nitrogen N1s peaks of *n*-butylamine (**12**) on (a) Au and (b) Pt.

and 71.1 and 74.4 eV ($Pt4f_{7/2}$ and $Pt4f_{5/2}$) are related to the substrates; the peaks corresponding to C1s and N1s are centered at 285 and 399 eV, respectively. The two other doublets correspond to the substrates, and O1s is observed at 532 eV. Observation of the substrate indicates that the organic layer is thinner than the analysis depth (of the order of 10 nm). Oxygen is mostly related to surface oxide and contamination. The N/C ratio should be related to the structure of the layer, but this ratio is very sensitive to surface contamination (adventitious hydrocarbon contamination is observed, although the samples were kept under argon between the preparation and the analysis, but untreated samples do not present any nitrogen peaks) and cannot be confidently used for the determination of the structure of the adlayer. In addition, examination of the carbon peak does not bring forward any evidence of a metal−carbon bond.

The specific nitrogen regions for *n*-butylamine (**12**) grafted on Au and Pt are shown in parts a and b of Figure 5, respectively. One can observe a component of the peak at low binding energy: 398.1 and 397.9 eV for *n*-butylamine (**12**) attached to Au and Pt, respectively. These components can be assigned to a nitride, therefore indicating the presence of a metal−nitrogen bond, as explained in the Discussion section. These results indicate that the organic groups are attached through the nitrogen, as previously supposed. The component at values close to 400 eV can be assigned to an amine group and would correspond to a C−N bond (butylamine presents an XPS peak at 398.9 eV[19a]), while the component at 402.0, clearly observed on Pt, could correspond to some amines protonated by the protons released during the oxidation process, as discussed above (ammonium chloride appears at 402 eV[19b]). As far as the attachment of the different classes of amines is concerned, N/C values on glassy carbon are reported in Table 7 altogether with the ratios previously measured by Porter;[7b] the values are in good agreement and indicate a larger amount of grafting for primary amines, a lower one (about half) for secondary amines, and nearly no grafting for tertiary amines. On Au and Pt, we have measured the ratios N1s/Pt and N1s/Au, where N1s is the component at 398 eV assigned to a nitrogen directly bonded to the metal. The ratio N1s/Au decreases from primary to secondary and tertiary amines, in which case it reaches a value close to zero; N1s/Pt also becomes negligible for tertiary amines.

The specific nitrogen regions for *n*-butylamine (**12**) grafted on Au and Pt are shown in parts a and b of Figure 5, respectively. One can observe a component of the peak

(19) (a) Lindberg, B. J.; Hedman, J. *Chem. Scr.* **1975**, *7*, 155. (b) Datta, M.; Mathieu, H. J.; Landolt, D. *Appl. Surf. Sci.* **1984**, *18*, 299. (c) Biwer, B. M.; Bernasek, S. L. *J. Electron Spectrosc. Relat. Phenom.* **1986**, *40*, 339. (d) Romand, M.; Roubin, M. *Analusis* **1976**, *4*, 308. (a) Barber, M.; Connor, J. A.; Guest, M. F.; Hillier, I. H.; Schwarz, M.; Stacey, M. *J. Chem. Soc., Faraday Trans. 2* **1973**, *69*, 551. (e) Leibsle, F. M.; Flipse, C. F. J.; Robinson, A. W. *Phys. Rev. B* **1993**, *47*, 15865. (f) Šiller, L.; Hunt, M. R. C.; Brown, J. W.; Coquel, J.-M.; Rudolf, P. *Surf. Sci.* **2002**, *513*, 78. (g) Hecq, A.; Delrue, J. P.; Hecq, M.; Robert, T. *J. Mater. Sci.* **1981**, *16*, 407.

Table 7. Nitrogen Region of XPS Spectra on Glassy Carbon, Gold, and Platinum

amine	N/C on glassy carbon[a]	N1s on Au (eV)	N/Au[b]	N1s on Pt (eV)	N/Pt[c]
n-butylamine (**12**)	3.4×10^{-2}	398.1	6.0×10^{-2}	397.9	2.4×10^{-2}
	3.7×10^{-2} [d]	399.8		399.8	
				402.0	
di-*n*-butylamine (**7**)	1.4×10^{-2}	399.5	2.4×10^{-2}	398.1	2.7×10^{-2}
				399.9	
				402.2	
n-butylmethylamine[d]	1.4×10^{-2}				
n-butylethylamine[d]	0.9×10^{-2}				
tri-*n*-butylamine (**3**)	ϵ[e]	no peak	ϵ[e]	no peak	ϵ[e]
n-butyldimethylamine[d]	ϵ[e]				

[a] Corresponding to the overall carbon and nitrogen peaks centered at 285 and 399 eV, respectively. [b] N1s component at 398 eV over Au $4f_{7/2}$. [c] N1s component at 398 eV over Pt $4f_{7/2}$. [d] Data from ref 7b. [e] Negligible.

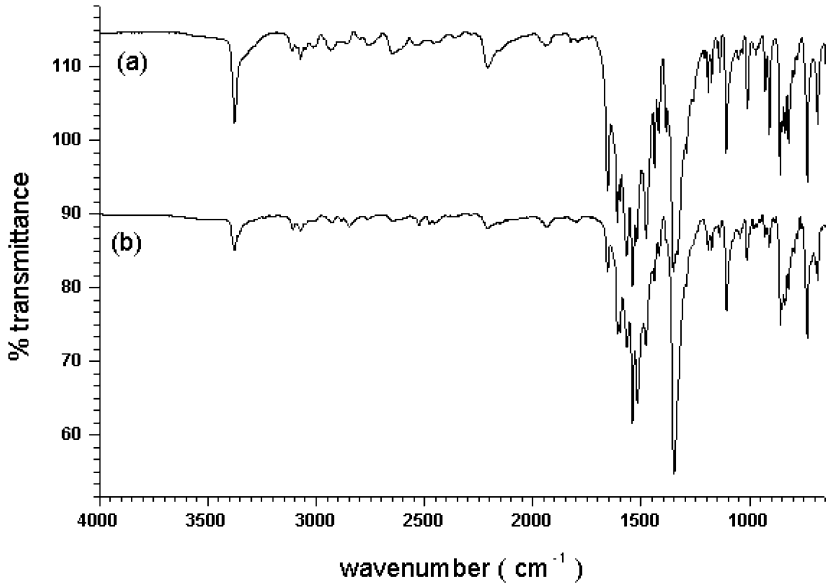

Figure 6. IR spectra of (a) 4-nitrobenzylamine (**16**) and (b) its (partly) di-N-deuterated analogue (**16D₂**).

at low binding energy: 398.1 and 397.9 eV for *n*-butylamine (**12**) attached to Au and Pt, respectively. These components can be assigned to a nitride, therefore indicating the presence of a metal−nitrogen bond, as explained in the Discussion section. These results indicate that the organic groups are attached through the nitrogen, as previously supposed. The component at values close to 400 eV can be assigned to an amine group and would correspond to a C−N bond (butylamine presents an XPS peak at 398.9 eV[19a]), while the component at 402.0, clearly observed on Pt, could correspond to some amines protonated by the protons released during the oxidation process, as discussed above (ammonium chloride appears at 402 eV[19b]). As far as the attachment of the different classes of amines is concerned, N/C values on glassy carbon are reported in Table 7 altogether with the ratios previously measured by Porter;[7b] the values are in good agreement and indicate a larger amount of grafting for primary amines, a lower one (about half) for secondary amines, and nearly no grafting for tertiary amines.

IR Analysis of the Pt Surface Modified with 4-Nitrobenzylamine (16). To confirm the attachment of 4-nitrobenzylamine to the surface of Pt, we examined the IRRAS spectrum of a Pt plate modified by electrolysis of 4-nitrobenzylamine ***Pt*16** at its peak potential for 600 s, and in hope to discriminate between the grafting of a radical and of a radical cation, we also examined the same Pt plate after modification with the N-deuterated analogue $ND_2CH_2C_6H_5NO_2$ ***Pt*16D₂**. The spectra of **16** and **16D₂** are presented in Figure 6, and those of ***Pt*16** and ***Pt*16D₂**, in Figure 7. These spectra are summarized in Table 8 altogether with the assignments of the bands.

These spectra confirm the attachment of **16** and **16D₂** to the Pt surface, upon electrochemical oxidation, through the presence of the strong asymmetric and symmetric stretching vibrations of the nitro group at 1540 and 1348 cm^{-1} (by comparison with 1511 and 1342 cm^{-1} for 4-nitro-α-methylbenzylamine[20c]) and the bands pertaining to the aromatic group. The spectrum of **16** presents thin NH_2 stretching at 3376 cm^{-1} (by comparison, the asymmetric and symmetric bands of liquid CH_3NH_2, $C_2H_5NH_2$, and *n*-$C_3H_7NH_2$ are located at 3399 and 3340, 3388 and 3322, and 3391 and 3325 cm^{-1}, respectively,[20d] and those of benzylamine[20a] appear at 3378 and 3289 cm^{-1}). The spectrum of ***Pt*16** shows a broad band at lower−3198 cm^{-1}−wavenumbers, indicating that the NH groups present on the surface are hydrogen-bonded and therefore close to one another, indicating a dense packing. The spectrum of partly deuterated **16D₂** (see the Experimental Section) presents two weak bands at 2526 and 2456 cm^{-1} which can be assigned to the symmetric and antisymmetric stretching of ND_2 by comparison with the values obtained for neat CH_3ND_2[20d] (2513 and 2442 cm^{-1}), $C_2H_5ND_2$ (2508 and 2432 cm^{-1}), and *n*-$C_3H_7ND_2$ (2514 and 2429 cm^{-1}). A

(20) (a) Leysen, R.; Van Rysselberge, J. *Spectrochim. Acta* **1963**, *19*, 243. (b) *The Aldrich Library of FTIR Spectra*, 2nd ed.; Sigma-Aldrich: Milwaukee, WI, 1997. (c) Leysen, R.; Van Rysselberghe, J. *Spectrochim. Acta* **1964**, *20*, 977. (d) Wolf, H.; Schmidt, U. *Ber. Bunsen-Ges. Phys. Chem.* **1964**, *68*, 579. (d) Wolf, H.; Schmidt, U.; Wolf, E. *Spectrochim. Acta* **1980**, *36A*, 899. (e) Gaver, R. W.; Murmann, R. K. *J. Inorg. Nucl. Chem.* **1964**, *26*, 881.

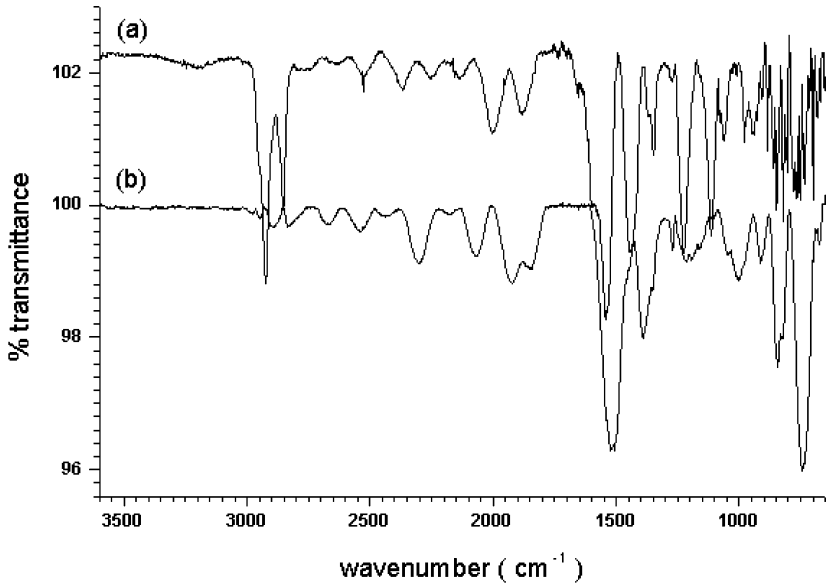

Figure 7. IRRAS spectra of a Pt plate modified with (a) ***Pt*16** and (b) ***Pt*16D$_2$**.

Table 8. IR Spectra[a] of 4-Nitrobenzylamine (16), Its N-Deuterated Analogue (16D$_2$), and the Same Molecules Grafted to Pt: *Pt*16 and *Pt*16D$_2$

	$C_6H_5CH_2NH_2$[b]	**16**[c]	***Pt*16**	**16D$_2$**[c]	***Pt*16D$_2$**
NH_2/ND_2	asym: 3378	3376 m	3198 w	2526 vw	2538 vw
	sym: 3289			2456 vw	2436 vw
CH arom	3024	3071 vw	3018[d]	3072 vw	*e*
CH_2/CD_2	2915	2932 vw	2923 s	2846 w	2070 w
	2855		2852 s		
NH deformation	1610	1611 m	1600 m	1610	*e*
aromatic ring	1580	1598 s	1593 m	1599 m	1521 vs
	1491	1568 s	1440	1567 s	
	1450	1521 s		1519 s	
		1476 m		1478 m	
NO_2		1540 s	1541 vs	1540 s	1542 vs
		1353 s	1348 m	1348 s	1389 m
CH out of plane	860	861 m	*f*	*f*	843 s
	736	730 m			742 vs

[a] Wavenumbers in cm^{-1}. [b] Pure liquid.[20b] [c] In KBr pellet. [d] Can be observed after enlargement of the spectrum. [e] Not observed. [f] Difficult to observe, as the spectrum is noisy in this region.

band at 2538 cm^{-1} can also be observed on the spectrum of ***Pt*16D$_2$**, indicating the presence of ND bonds on the surface. As stated above, the XPS spectra on Pt indicate that some of the amines on the surface are protonated; this could correspond to a band observed at 2300 cm^{-1} on the spectrum of ***Pt*16**. The CH_2 stretching is observed as a weak band at 2932 cm^{-1} on the spectrum of **16** but as two strong bands at 2923 and 2852 cm^{-1} on the spectrum of ***Pt*16**. This increased intensity can be assigned to the relative orientation of the CH bonds which should be close to the surface normal in accordance with the selection rules for surface spectra. A molecular model shows that this is indeed the case for one of the CH bonds. The spectrum of ***Pt*16D$_2$** shows a nearly complete disappearance of the CH bands but an appearance of a small band at 2070 cm^{-1}; we have assigned this small band to the formation of CD bonds by comparing it with the C−D bands of C-deuterated ethylenediamine[20e] located at 2100 cm^{-1}.

Discussion

All the data obtained in this paper—cyclic voltammetry (through the observation of the reporting nitro group and through the slowing of the electron transfer on modified electrodes), XPS (through the observation of nitrogen on the surface), and IRRAS (through the observation of the aromatic and nitro groups of the nitrobenzylamino group)—point to the attachment of the amino groups to C, Au, and Pt surfaces.

Investigation of the different classes of amines in DMF on carbon electrodes shows that tertiary and secondary amines follow an EC mechanism. With these amines, it is always possible through an increase of the scan rate to observe the radical cation, the first intermediate of the oxidation. With primary amines, the radical cation is too unstable to be observed, but the value of α close to 0.5 does not point to a concerted mechanism[21] where there would be no radical cation on the oxidation path (a much lower value of α = 0.2−0.3 would be expected for a concerted process). Therefore, an EC mechanism is also likely involved in the oxidation of primary amines. The chemical reaction following the electron transfer is first order, the rate constant of this reaction being only slightly larger for secondary amines than for tertiary amines. This means that the stability of the radical cations of secondary and tertiary amines is similar. The follow-up reaction is the loss of a hydrogen α of the nitrogen for the three classes of amines, as observed in DMF for secondary and tertiary amines.

As indicated in the Introduction, either the radical cation or the radical could be responsible for the attachment of the organic group to the surface. This investigation confirms at least for tertiary and secondary amines the existence of the radical cation, and for primary amines, there is no sign of an electron transfer concerted with the loss of a proton, excluding reaction **R2** in Scheme 11. Therefore, it is not possible to rule out the possibility that the radical cation binds to the surface (reaction **R5**, Scheme 11) on the sole analysis of the voltammograms.

In DMF, where the attachment to the surface is minimized, the lifetime of the radical cation is <0.2 ms for primary amines, 4 ms for secondary amines, and 13 ms for tertiary amines. This lifetime is related to the rate of proton loss from the radical cation. The same order of deprotonation rates can be assumed in ACN. Therefore, the radical would be formed faster for primary amines than for secondary and tertiary amines. In the context of electrochemistry where the products diffuse from the

(21) (a) Savéant, J. M. *Adv. Phys. Org. Chem.* **2000**, *35*, 117. (b) Pause, L.; Robert, M.; Savéant, J. M. *J. Am. Chem. Soc.* **2001**, *123*, 4886.

Scheme 11

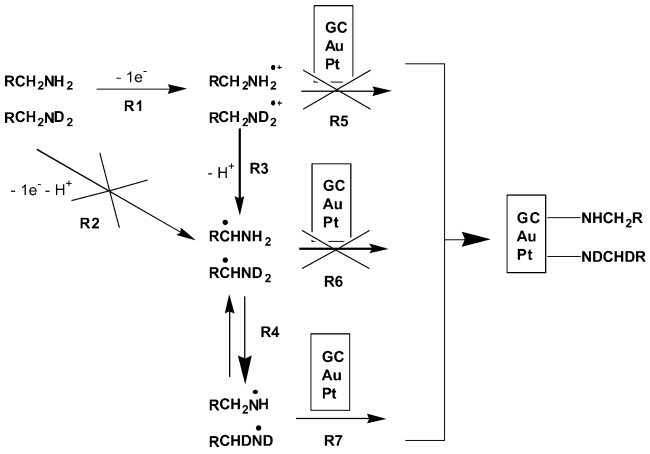

electrode to the solution, the radical obtained from primary amines is formed closer to the electrode than that of secondary or tertiary amines. This strongly supports the fact that the radical is the species which binds to the surface. However, it is not possible, from purely electrochemical data, to reject entirely a mechanism where the radical cation of primary amines would bind faster to the surface than that of secondary or tertiary amines for steric and electronic reasons (increasing the number of electron donating alkyl groups from primary to tertiary amines would increase the positive charge of the radical cation and disfavor the attack of electron rich carbon or metal surface). Fortunately, the IR data permit support of the radical mechanism. These data indicate that starting from $D_2NCH_2C_6H_4NO_2$ **16D₂** one observes on the spectrum of ***Pt*16D₂** the presence of ND bonds and of a small band assigned to CD bonds but mostly the disappearance of the strong CH bands which are observed in ***Pt*16**. The observation of a CD bond clearly indicates that the radical cation is not the species which attaches to the Pt surface (excluding reaction **R5**); if the direct binding of the radical cation was occurring, there would be ND bonds but no CD bonds. The most likely pathway leading to a surface attached amine with both ND and CD bonds is therefore **R1** + **R3** + **R4** + **R7** (Scheme 11), already proposed above on the basis of considerations on the stability of radicals. This reaction path involves the formation of a radical cation (**R1**), in agreement with the electrochemical data; the deprotonation—observed as a first-order reaction following the electron transfer in cyclic voltammmetry—of a CH bond was observed with tertiary and secondary amines (**R3**) and the shift of the equilibrium of Scheme 6 to the amino radical (**R4**) which finally binds to the surface, as discussed below (**R7**).

As far as the attachment of amines to carbon is concerned, it is not possible to distinguish the carbon−nitrogen bonds of the amine from that responsible for the attachment, but on Au and Pt, XPS spectra clearly evidence the presence of a nitride (398.1 and 397.9 eV for Au and Pt, respectively) which can be assigned to the metal−nitrogen bond. For example, N1s peaks are observed at 397.3 eV for iron nitride,[19c] 396.8 eV for CrN,[19d] 396.5−396.8 eV (depending on the coverage) for chemisorbed nitrogen on Cu(110),[19e] and 396.6 eV for Au nitrides (Au_xN) obtained by irradiation of Au(110) surfaces by nitrogen.[19f] On Pt surfaces sputtered with nitrogen ions, the presence on platinum nitride has been associated with a low binding energy component of the N1s peak at 398.5 eV[19g] and a peak for $Pt4f_{7/2}$ at 72.13 eV (by comparison with 71.19 eV for pure Pt). These data indicate that the binding energies of both Pt and nitrogen are very similar for the amine modified surfaces and for Pt nitride. This platinum nitride is characterized by a limited metal to nonmetal charge transfer. Data are lacking for the binding energy of Au in Au nitride, but the similarity of the values obtained for N1s also point to a covalent Au−N bond.

A possible alternative to a covalent bond could be a weaker bond similar to that involved in self-assembled monolayers of thiols on Au. It would be unlikely that such weakly bonded layers would resist ultrasonic rinsing; indeed, amines do not form stable, close-packed, ordered monolayers on a Au(111) surface.[22]

This demonstrates that grafting indeed takes place through the nitrogen on Au and Pt; it is likely that the same reaction takes place on carbon. As a consequence of the proposed mechanism, **R1** + **R3** + **R4** + **R7**, polyethyleneimine[8] which is formed on Pt by the oxidation of neat ethylenediamine should be also attached to the surface by a covalent metal−nitrogen bond. The electrochemical oxidation of amines therefore provides an interesting method for the attachment of polymers on metal surfaces, provided the oxidation of the amine is easier than that of the metal.

One can compare the attachment of the different classes of amines on carbon. Cyclic voltammetry on carbon indicates that the attachment reaction of primary amines is much more efficient than those of secondary and tertiary amines. This is also observed by measuring ΔE_p (Table 4), which is a measure of the rate of electron transfer through the adlayer, by XPS (Table 7), and by cyclic voltammetry of the reporting nitro group (Table 6). The values of surface concentrations obtained by this method are close but always smaller than that of the most compact layer which can be calculated from molecular models (mostly if one takes in account the roughness of the surface). From these data, the coverage of the adlayer appears to be in the following order: primary amines > secondary amines > tertiary amines, with the binding of this last class of amines being negligible. Within the precision of the different methods, there is no large difference between C, Au, and Pt concerning the surface coverage of amino groups, although the surface coverage seems slightly larger on Pt, but this could be related to the roughness of the surface, as the values are reported to geometrical and not to real surfaces.

Conclusion

The attachment of amino groups to the surface of C, Au, and Pt electrodes is confirmed by the following different methods: cyclic voltammetry, XPS, and IRRAS. It is possible to observe the XPS signature of the metal−nitrogen bond, indicating that the attachment of the organic group is not a mere physisorption. The mechanism leading to this binding of the amino group has been unraveled. Careful investigation of the cyclic voltammetry of aliphatic amines indicates that the first intermediate is a radical cation which deprotonates to give a radical along a sequential pathway. It is this radical that binds to the surface of the electrode. The reaction path to the grafting of amines should therefore follow reactions **R1** + **R3** + **R4** + **R7** of Scheme 11. This is in agreement with other grafting reactions where radicals react with the electrode surface.

(22) (a) Ulman, A. *An Introduction to Ultrathin Organic Films: From Langmuir-Blodget to Self-Assembly*; Academic Press: New York, 1991, p 1. (b) Bain, C. D.; Evall, J.; Whitesides, G. M. *J. Am. Chem. Soc.* **1989**, *111*, 7155. (c) Xu, C.; Sun, L.; Crooks, R. M. *Anal. Chem.* **1993**, *65*, 2102.

Experimental Section

The amines used in this study were obtained from Aldrich and used as received except the secondary and tertiary nitrobenzylamines which were prepared according to ref 23.

4-Nitrobenzylamine (**16**) was obtained from the commercial hydrochloride ammonium salt by dissolving 500 mg of it in 10 mL of water, adding 0.18 mL of concentrated (40%) NaOH, extracting with 3 × 10 mL of toluene, drying the organic layer, and evaporating under vacuum. The amine is not very stable and was kept under argon at −20 °C and used as rapidly as possible. The deuterated analogue was prepared under the same conditions using D_2O and a few drops of DCl and NaOD. The hydrochloride was left 3 days in contact with D_2O under argon and finally refluxed for 6 h. The deuteration was checked by NMR (the broad NH_2 peak at 2.0 ppm observed for **20** in dry DMSO-d_6 disappears) and by mass spectroscopy. The ratio of the peaks at *m*/*e* 154 and 152 never exceeded 30% despite many experiments.

ACN (Merck Uvasol) and DMF (SDS for peptide synthesis) were reagent grade quality and used without further purification. NBu_4BF_4 was from Fluka (puriss, 99%).

The electrochemical conical cell which can be used for three electrodes was equipped with a methanol jacket, allowing the temperature to be fixed by means of a thermostat (10 °C in all the cases studied). For cyclic voltammetry experiments, the working electrode was in all cases a glassy carbon disk with a diameter of 1 mm. This was polished by using a 1 μm diamond paste. The counter electrode was a Pt disk with a diameter of 1 mm. All the potentials are reported versus an aqueous saturated calomel electrode isolated from the working electrode compartment by a salt bridge. The cyclic voltammetry apparatus was composed of a home-built solid-state amplifier potentiostat with positive feedback iR drop compensation and a Tacussel GSTP 4 generator. The voltammograms were displayed on a Tektronix (2212) instrument. Electrolyses were carried out in the same electrochemical cell as cyclic voltammetry experiments using a PAR 273A potentiostat. A graphite rod was used as the working electrode and a Pt wire as a counter electrode isolated from the anodic compartment.

Electrografting experiments were carried out with a glassy carbon disk (diameter, 3 mm), a Pt disk (diameter, 1 mm), and a Au disk (diameter, 1 mm) as working electrodes.

The XPS spectrometer equipment has been previously described.[10b] The IR spectrometer was a Nicolet Magna 860 and was used in the reflection mode for the spectra of Figure 6. The same Pt 35 × 15 mm^2 was used for recording the background and the spectra of ***Pt*16** and ***Pt*16D$_2$**, taking great care that the plate be exactly at the same position for every spectrum. Before each experiment, it was polished with 1 and 0.25 μm diamond paste and carefully rinsed in ACN.

Acknowledgment. We are grateful to P. Bargiela for recording the XPS spectra. Financial support from the DGI (MEC of Spain) through project BQU2003-05457 is gratefully acknowledged.

Supporting Information Available: An analysis and figures of the electrochemical data for **5** and **12**. This material is available free of charge via the Internet at http://pubs.acs.org.

LA049194C

(23) Avery, M. A.; Bhattacharyya, S.; Neidigh, K.; Williamson, J. *J. Chem. Soc., Perkin Trans. 1* **1998**, 2527.